THE ASTROPHYSICAL JOURNAL, 413:548–561, 1993 August 20

HIGH-DISPERSION SPECTROSCOPY OF GIANTS IN METAL-POOR GLOBULAR CLUSTERS. I. IRON ABUNDANCES

DANTE MINNITI[1]
Steward Observatory, University of Arizona, Tucson, AZ 85721
DOUG GEISLER
Cerro Tololo Inter-American Observatory, 950 North Cherry Avenue, Tucson, AZ 85719
RUTH C. PETERSON
Lick Observatory, University of California, Santa Cruz, CA 95064
AND
JUAN J. CLARIA[1]
Observatorio Astronomico, Laprida 854, 5000 Cordoba, Argentina
Received 1992 October 19; accepted 1993 February 23

ABSTRACT

We determine iron abundances for an average of two to three giant stars in each of eight metal-poor Galactic globular clusters. We present equivalent width measurements derived from high-resolution ($\lambda/\Delta\lambda \sim 25{,}000$), high S/N ratio ($45 \leq S/N \leq 100$ per pixel) echelle CCD spectra. The abundances are determined using line analysis via latest generation model atmospheres and synthetic spectrum techniques. We derive the following [Fe/H] values (relative to a solar Fe abundance of 7.5): -2.17 ± 0.05 (standard error of the mean, based on two stars) for M68, -1.71 for NGC 4833 (one star), -1.59 for NGC 6144 (one star), -1.99 ± 0.01 for NGC 6397 (six stars), -1.58 ± 0.04 for NGC 6752 (three stars), -1.96 ± 0.04 for M55 (two stars), -2.23 ± 0.04 for M15 (two stars), and -2.10 ± 0.08 for M30 (two stars), with no evidence for intracluster metallicity variations. We estimate the total errors to be of order 0.15 dex, including internal and external sources. These values are in excellent agreement with previous results of similar high quality. The low end of the globular cluster metallicity scale is now well established by such spectroscopic data and support the Zinn (1985) scale, with an error of <0.15 dex. The Washington scale of Geisler et al. (1991), is also generally supported, but the errors are larger (~ 0.23 dex), as expected from the high reddening and reduced metallicity sensitivity of this photometric system at these low abundances. However, several of the clusters suggested by the Washington photometry of Geisler et al. (1992) as being more metal-poor than their Zinn (1985) values are instead found to have intermediate metallicities. We find that the mass-metallicity limit imposed by assuming the self-enrichment of metal-poor globulars by supernovae provides a boundary that is in good agreement with the observed distribution.

Subject headings: globular clusters: general — stars: abundances — stars: giants — stars: Population II

1. INTRODUCTION

How firmly established is the metallicity scale for globular clusters? A decade ago, controversy raged over the metallicity of the most metal-rich clusters, a controversy that was decided only after the very high quality data afforded by the advent of high signal-to-noise ratio, high-resolution CCD spectra (hereafter denoted as HDS) of individual giants was obtained. Recently, hints that the metal-poor end of the scale may not be as firm as generally believed have surfaced. For example, Suntzeff, Kraft, & Kinman (1988) derived a value for the metallicity of NGC 5053, the most metal-poor cluster on Zinn's (1985, hereafter Z85) widely accepted metallicity scale, that was 0.4 dex larger than the Zinn value, although the Armandroff, Da Costa, & Zinn (1992) value for this cluster is only about 0.2 dex larger than Z85. Alternatively, Peterson, Kurucz, & Carney (1990) found an abundance for M92 that was only about half that of most previous estimates; and Geisler, Minniti, & Claria (1992, hereafter GMC) suggested that several clusters could be substantially more metal-poor than given by the Zinn scale. Again, definitive answers must come from the high-quality spectroscopic observations of individual giants that are now well within reach of 4 m class telescopes, at least for the brighter giants in nearby clusters.

Indeed, such HDS observations have been obtained for several metal-poor clusters in recent years, as exemplified by the work of Gratton and collaborators (Gratton & Ortolani 1989, hereafter GO) and Sneden et al. (1991, hereafter SKPL). These observations have so far confirmed the Zinn scale, but only a small number of clusters has been investigated and much work remains to corroborate and supplement these results. We emphasize here that the previous generation of results based on photographic echelle work is generally of insufficient resolution and/or signal-to-noise ratio (especially) to be very reliable. Thus, HDS here implies *only high-quality data.*

In this paper, we attempt to tighten the low end of the metallicity scale, and to examine more closely the metal-poor tail of the Galactic globular clusters, using HDS of single giants. In order to accomplish this, a large and homogeneous sample is required. Only a small percentage of the known globulars have had accurate determinations of their chemical composition via HDS. A much larger fraction have photometric or low-resolution spectroscopic metallicity determinations for single stars, techniques which have the advantage of being much more efficient, but which need to be calibrated

[1] Visiting Astronomer, Cerro Tololo Inter-American Observatory, NOAO.

with HDS. The present sample greatly improves the situation at the metal-poor end, where many techniques lose sensitivity and the calibrations might be questionable. We were especially motivated in this regard by our recent results based on Washington photometry (GMC). In that paper we found that, although the Washington and Zinn scales were in good general agreement, there were several metal-poor clusters for which we derived metallicities substantially less than those given by Zinn, in particular M68, NGC 2298, NGC 4833, NGC 5897, and NGC 6101. However, the Washington abundances were quite uncertain due to the high reddening and photometric error sensitivities of the system for cool, metal-poor stars. Subsequently, though, an intermediate metallicity for NGC 2298 has been obtained from HDS (McWilliam, Geisler, & Rich 1992), so that similar studies for these other clusters are also of interest for checking their metallicities.

Such studies are also important for investigating possible chemical composition differences between halo globular clusters and halo field stars. It is not difficult to imagine a scenario in which the chemical history of these two entities was distinct. However, various theories for halo field and globular cluster formation predict similar chemical compositions, and indeed a common origin. In the Fall & Rees (1985) scenario, the field halo stars are the debris from a much larger globular cluster system destroyed by various processes (dynamical friction, tidal limitations, evaporation, and disk shocking). Zinnecker et al. (1988) and Freeman (1990) proposed that globular clusters are the cores of nucleated blue dwarf spheroidal galaxies accreted by the parent galaxy, while the field population was formed from the dissolution of the remainder of the dwarfs. Dynamical processes during the (especially early) lifetime of globulars could supply the halo with stars (Chernoff & Weinberg 1990), and such disruption processes are selectively dependent on location within the Galaxy. Detailed chemical abundances offer a powerful method of investigating whether the halo field and cluster stars both come from the same parent population. Laird et al. (1988) and Ryan & Norris (1991) demonstrate that, while there is a significant lack of metal-poor clusters with respect to the halo field star metallicity distribution function, both distributions do have the same peak. Thus, it is particularly important to confirm the metallicity scale for the most metal deficient clusters.

This paper presents Fe abundances for eight metal-poor Galactic globular clusters. We describe the observational, reduction and analysis procedures in §§ 2 and 3. Our results are compared to previous values in § 4, and we discuss a number of implications in § 5. Finally, we give a summary of our work in § 6.

2. OBSERVATIONS AND DATA REDUCTION

The selected clusters were those observed by GMC. We attempted to obtain observations for all 10 of their clusters; however, time and weather limited us to only six of these; NGC 4590 (M68), 4833, 6397, 6809 (M55), 7078 (M15), and 7099 (M30). Subsequently, NGC 2298 has been observed and analyzed (McWilliam et al. 1992). We also obtained observations of two additional clusters—NGC 6144 and 6752.

All of these clusters have various metallicity estimates, ranging from color-magnitude diagram (CMD) morphology to HDS, which place them among the metal-poor tail of the globular cluster distribution. Several of these clusters, notably M68, M30, and especially M15 and NGC 6397, are prototypical metal-poor clusters which are used to calibrate a number of metallicity indices. In addition, most of these clusters are nearby and contain a selection of bright giants which are amenable to HDS. Note, however, that a wide range of published metal abundances can be found for some of these clusters. Perhaps the most extreme case is M55, where the photographic echelle spectra of Pilachowski, Sneden, & Green (1984) yielded $[Fe/H] = -1.3 \pm 0.1$, while GMC find -1.95 ± 0.3.

The observed stars all have good quality BV photometry, as well as CMT_1T_251 photometry. The former data show the stars all lie along the upper giant branch, within ~ 1 mag of the tip, while the latter data indicate they are all metal-poor giants. Thus, these two photometric criteria strongly demonstrate cluster membership. The existing radial velocity information also confirms membership. These stars are isolated on the finding charts, with no contaminating neighbors, and all lie in the outer parts of the clusters. Some observed parameters for the sample stars are listed in Table 1. The reddenings and distances come from Armandroff (1989). While the candidate stars span a wide range in M_V and $(B-V)_0$, they all have $T_{\rm eff} \geq 4300$ K, hot enough to circumvent the variety of problems plaguing abundance determinations for cooler giants.

The observations were done during three nights in 1990 July and one night in 1992 May at the Cerro Tololo Inter-American Observatory 4 m telescope. We used the 31.6 echelle plus long camera with the Thompson or Tek chips, which provides extended wavelength coverage at high resolution. The effective resolution was 27,000 (0.23 Å at 6300 Å) on three of the nights and 22,000 on the remaining night, with $\sim 80\%$ complete coverage from 5500 to 6800 Å. The highest resolution data had a FWHM of ~ 4 pixels. The seeing was variable between 1″ and 3″. The slit width was 1.″3 on nights 1, 3, and 4, and 1.″6 on night 2. Th-Ar comparison lamps were taken to corroborate the wavelength calibration done from spectral features themselves. We also observed rapidly rotating early-type stars at different air masses bracketing the range of air-masses covered by the program stars. Division by these early-type stars accounts for telluric lines. The run was during gray time, with the moon far from the targets in the sky. No additional correction for scattered light, other than sky subtraction, was needed.

The exposure times, listed in Table 1, were no longer than 40 minutes. The individual spectra were co-added after the wavelength calibration. The intensity achieved varies by a factor of ~ 1.4 from the blue to the red end of every order. There is also a variation in S/N as a function of order number, the bluest orders having higher values. The mean S/N per extracted pixel, i.e., perpendicular to the dispersion, for each spectrum in the eighth order region around the O [I] 6300 Å line is listed in Table 1. Note that, due to the large FWHM in pixels, the S/N per resolution element is about twice this value.

All of the data reduction was done in IRAF with the ECHELLE package. Bad pixels and cosmic rays were fixed by interpolating between neighboring pixels. There was no problem identifying such defects due to the high resolution.

The wavelength calibration was done using typically 50 known features in the 19 echelle orders. The equivalent widths (EW) were measured interactively with the SPLOT package, using a Gaussian that fitted each line with the extremes selected from the local continuum. Most of the lines were isolated, but occasional blends were fitted with multi-Gaussians. No flux calibration was applied. The continuum was determined by interactive fitting a spline of high order. For the stars in the present study, the continuum is well defined, since there are

TABLE 1

PHOTOMETRY FOR METAL-POOR GLOBULAR CLUSTER STARS

M/NGC	Star	ID Source[a]	Exposure time (s)	S/N	T_{Wash}[b]	$T(V-K)$[c]	V	$(B-V)_0$	$E(B-V)$[b]	log g[d]	$m-M$[e]
M68	53	1	3 × 2000	65	4350	4372	12.76	1.27	0.06	0.8	15.14
M68	260	2	3 × 1800	65	4330	4329	12.52	1.22	0.06	0.7	15.14
M30	D	3	3 × 1600	40	4570	...	12.81	1.03	0.04	1.1	14.65
M30	157	3	3 × 2000	65	4600	...	12.94	1.01	0.04	1.1	14.65
M15	II-75	4	4 × 1800	45	4460	4416	13.00	1.14	0.10	0.9	15.40
M15	s6	4	4 × 1800	45	4500	4460	13.40	1.09	0.10	1.0	15.40
M55	283	2	3 × 1600	90	4690	...	12.75	1.08	0.06	1.0	13.94
M55	76	5	3 × 2400	75	4710	...	12.55	0.92	0.06	1.4	13.94
N6144	152	6	4 × 2400	65	4320	...	14.06	1.20	0.33	0.9	16.24
N4833	13	7	3 × 1900	65	4500	...	12.80	1.09	0.32	1.0	14.99
N6397	302	8	1 × 900	90	4420	...	10.36	1.19	0.18	0.9	12.44
N6397	603	9	1 × 900	90	4460	4374	10.35	1.15	0.18	0.9	12.44
N6397	669	9	1 × 900	90	4560	4420	10.50	1.10	0.18	1.0	12.44
N6397	331	9	1 × 900	90	4250	...	10.06	1.34	0.18	0.5	12.44
N6397	468	9	1 × 900	90	4800	...	10.56	0.87	0.18	1.5	12.44
N6397	428	9	1 × 900	30	4780	...	10.56	0.87	0.18	1.5	12.44
N6752	284	10	1 × 1800	70	4470	...	11.38	1.19	0.04	0.9	13.30
N6752	36	10	1 × 1800	70	4470	...	11.51	1.15	0.04	0.9	13.30
N6752	29	10	1 × 1800	70	4560	4253	11.75	1.12	0.04	1.0	13.30

[a] SOURCES.—(1) Alcaino 1977a; (2) Harris 1975; (3) Alcaino & Liller 1980; (4) Sandage 1970; (5) Alcaino 1975; (6) Alcaino 1980; (7) Alcaino 1971; (8) Alcaino 1977b; (9) Cannon 1974; (10) Alcaino 1972.

[b] From Geisler et al. 1992.

[c] From Frogel et al. 1983.

[d] From interpolation in Fig. 10 of Carbon et al. 1982.

[e] From Armandroff 1989, assuming $V_{hb} = 0.46$.

very few lines and most of them are weak. Any systematic effect in the fitting of the continuum would show as a systematic difference of the measured EW versus those from other authors. However, as discussed below, we find excellent agreement between our measurements and those of other HDS studies.

The division by a rapidly rotating star was successful at eliminating telluric lines except in the case of M15 star II-75, where telluric lines in the eighth and 13th orders did not divide out simultaneously. The scale factor was then chosen to eliminate completely the telluric lines in the eighth order, where the 6300 Å oxygen line is. In all cases, the scale factor was roughly proportional to the air mass. Representative spectra in the region near 6300 Å are shown in Figure 1.

We restricted our analysis to the spectral range 5500–6500 Å. Typically, this included 45–60 good Fe I lines with excitation potentials (EP) between 0.7 and 5 eV, and about three to six Fe II lines per spectrum. Table 2 lists all the lines measured, as well as the adopted values of log gf and EP for each line. The gf-values are from Peterson & Carney (1989) and are laboratory values. The solar Fe abundance selected is that of Holweger et al. (1990, 1991), log N(Fe) = 7.5 on a scale where log N(H) = 12.0. Thus, if a different value is preferred, the derived Fe abundance will change accordingly. For example, our derived Fe abundances will be 0.17 dex higher than if we had assumed the solar Fe abundance given by Anders & Grevesse (1989), which has been used in many previous analyses. However, most recent analyses, e.g., SKPL and McWilliam et al. (1992), have adopted a value similar to ours. This illustrates that substantial uncertainties still exist in Fe abundance work. The goal of this paper is to provide an abundance ranking and absolute values of metal abundance. The ranking is necessarily more precise than the absolute values, which depend on the adopted solar composition.

In Figure 2, we compare our measured EW with those measured by other authors with similar HDS. There we plot the lines in common with GO, Peterson et al. (1990), and SKPL. We have included the metal-poor halo giant HD 122563 which was observed and reduced in the same way as the globular cluster giants. The mean difference with SKPL is δ_{EW} = EW (comparison) − EW (this paper) = -0.24 ± 0.56 mÅ for 23 lines in common; the mean difference with Peterson et al. (1990) is $\delta_{EW} = 0.19 \pm 0.26$ mÅ for 18 lines. Both comparisons show excellent agreement. Note that the differences for these two comparisons are of opposite sign. There is a systematic difference with GO of $\delta_{EW} = 1.02 \pm 0.90$, and a larger scatter,

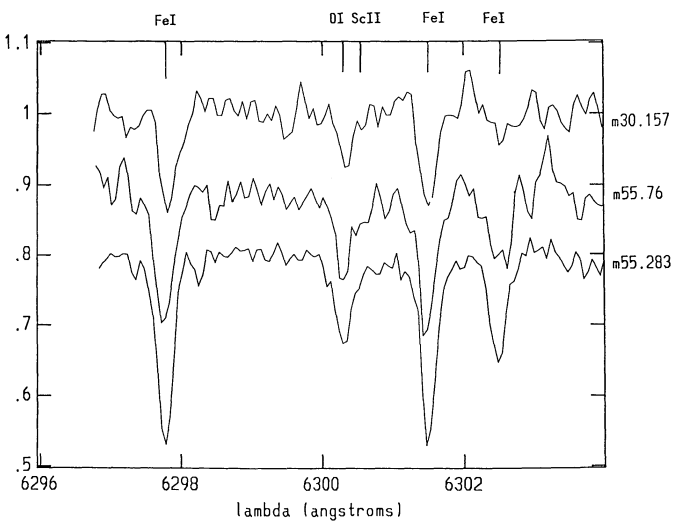

FIG. 1.—Representative spectra in the vicinity of the [O I] line at 6300.3 Å are shown in the same residual intensity scale, displaced vertically by 10%. From top to bottom, the stars are M30 star 157, M55 star 76, and M55 star 283. Absorption features are identified at the top.

1993ApJ...413..548M

TABLE 2

EQUIVALENT WIDTH MEASUREMENTS FOR Fe I AND Fe II LINES

Lambda	loggf	EP	M15 II75	M15 s6	M30 157	M30 sd	M55 283	M55 s76	M68 260	M68 53	N4833 13	N6144 152	N6397 603	N6397 669	N6397 302	N6397 331	N6397 468	N6397 428	N6752 29	N6752 36	N6752 284
550.6778	0.990	-2.797	----	----	----	----	17.40	----	----	----	----	----	----	----	----	----	----	----	----	----	----
552.5539	4.230	-1.260	----	----	----	----	7.64	----	----	----	----	----	----	----	----	----	----	----	----	----	----
553.4847	3.245	-2.996	----	----	2.50	----	----	----	2.67	3.41	4.47	5.86	4.50	4.77	4.57	----	----	----	6.44	6.27	6.10
554.3147	3.695	-1.500	----	----	----	----	1.69	----	----	----	----	----	0.79	----	----	----	----	----	----	----	----
554.3937	4.217	-1.070	----	1.98	----	----	----	----	1.29	1.41	3.11	3.48	1.88	----	----	----	----	----	3.86	4.68	----
554.6500	4.371	-1.240	----	----	----	----	----	----	2.04	----	----	4.97	----	----	2.09	----	----	----	----	2.57	----
555.4882	4.548	-0.414	----	1.77	2.02	----	3.32	----	2.03	1.46	4.84	----	2.51	----	----	----	----	----	5.41	5.62	4.55
556.0207	4.434	-1.120	----	----	----	----	----	----	1.97	----	----	----	2.02	----	0.90	1.05	----	----	----	2.64	1.70
557.6090	3.430	-0.930	----	5.35	4.47	----	8.12	----	7.06	6.09	----	9.43	7.92	6.97	7.98	9.61	4.49	----	10.40	11.80	10.50
558.6756	3.368	-0.180	----	10.70	9.42	----	12.60	----	12.00	10.80	13.60	12.00	11.60	11.20	11.90	15.40	10.50	5.55	13.90	13.70	15.40
563.8262	4.220	-0.800	2.74	0.57	1.44	1.74	1.23	----	----	1.49	3.47	5.02	2.88	2.52	2.55	3.33	3.53	----	4.20	5.77	5.73
566.2515	4.178	-0.541	2.74	2.69	2.37	----	4.26	6.45	2.96	3.03	15.00	3.56	3.80	3.48	4.59	3.69	1.24	----	7.47	6.92	7.40
568.6524	4.548	-0.620	1.37	1.27	2.16	2.06	----	----	----	0.78	2.32	3.58	2.41	2.49	2.08	1.90	----	----	4.75	5.11	4.44
570.1545	2.559	-1.565	5.37	5.12	4.91	5.04	7.52	7.24	6.26	5.38	8.00	10.20	6.74	6.62	7.35	10.30	4.33	----	9.05	9.43	10.80
573.1762	4.256	-1.230	----	----	----	1.61	----	----	----	----	----	----	----	----	----	----	----	----	----	----	----
581.6367	4.548	-0.653	----	0.77	1.11	----	1.59	----	1.47	0.97	4.39	2.67	1.45	0.80	1.67	1.85	1.63	----	3.60	4.75	4.94
585.9578	4.548	-0.398	----	----	----	----	2.61	1.28	1.16	1.41	2.65	3.30	1.51	1.33	1.78	3.21	1.36	----	4.85	4.47	4.39
586.2353	4.548	-0.058	1.14	0.93	1.42	2.96	3.22	2.14	1.77	2.26	4.25	4.80	3.15	3.25	2.75	2.45	1.54	----	6.38	6.05	6.22
588.3813	3.960	-1.290	----	1.32	2.17	0.67	1.96	----	2.58	2.18	0.35	2.17	1.07	1.91	----	----	----	----	4.28	4.82	----
593.0173	4.652	-0.196	1.60	2.36	----	1.72	3.27	2.48	2.31	2.59	2.50	3.71	2.63	2.58	2.93	4.02	1.83	----	5.20	5.83	5.66
593.4653	3.929	-1.100	1.66	1.57	1.15	0.46	3.19	1.44	2.13	1.07	3.24	3.14	3.04	3.41	3.48	5.37	1.92	----	5.67	5.79	6.43
594.3577	2.198	-4.523	----	----	----	----	0.51	----	----	----	----	----	----	----	----	----	----	----	----	----	----
595.2716	3.984	-1.370	----	----	----	1.40	1.59	----	----	----	----	----	----	----	----	----	----	----	----	----	----
595.6692	0.859	-4.608	4.05	----	----	4.23	7.71	4.55	----	5.64	----	----	----	----	----	----	----	----	----	----	----
597.6775	3.943	-1.310	----	----	----	----	----	----	----	2.13	----	----	----	----	----	----	----	----	----	----	----
598.3673	4.548	-1.878	----	----	----	----	1.63	1.94	----	----	----	----	----	----	----	----	----	----	----	----	----
598.4814	4.733	-0.343	----	----	----	----	2.86	2.19	----	----	----	----	----	----	----	----	----	----	----	----	----
598.7066	4.795	-0.556	----	----	----	----	1.24	0.95	0.85	1.53	2.05	1.62	2.03	----	1.65	1.53	----	----	4.28	3.39	3.84
599.1376	3.153	-3.557	----	1.20	0.86	0.95	0.94	----	1.39	0.61	----	2.06	1.55	1.58	1.26	----	----	----	2.93	2.74	2.79
600.3010	3.882	-1.089	----	2.23	----	2.80	3.47	2.19	3.30	2.16	4.63	4.80	3.42	2.82	4.10	5.24	2.13	----	6.47	6.61	6.57
600.5543	2.588	-3.192	----	----	----	----	1.89	1.16	----	1.91	----	----	1.08	1.21	0.94	1.15	----	----	3.39	2.82	2.69
600.7960	4.652	-0.966	----	1.11	0.66	----	0.70	----	0.54	2.68	----	----	----	----	1.39	1.30	----	----	2.76	3.55	3.23
600.8554	3.883	-1.078	2.74	1.72	2.86	1.18	3.81	2.85	2.99	1.89	5.01	5.86	4.19	3.50	4.05	6.69	2.06	----	7.37	7.33	7.88
601.2206	2.223	-4.090	----	0.65	----	0.99	1.82	----	0.68	----	1.61	2.77	0.60	0.61	0.77	1.61	----	----	1.72	2.84	2.54
602.0170	4.607	-0.244	----	1.48	1.73	1.94	3.78	2.78	2.51	1.71	5.41	5.65	3.92	2.98	3.21	5.00	2.31	----	7.21	7.81	8.05
602.4049	4.548	-0.089	3.62	2.86	2.91	1.42	5.52	4.21	3.73	2.12	5.92	----	5.05	5.51	4.63	5.30	3.07	2.03	7.42	7.97	7.68
602.7050	4.076	-1.140	----	----	0.60	----	2.13	----	0.77	1.16	3.00	4.40	----	2.27	2.94	2.25	1.49	----	3.87	4.85	4.67
605.5992	4.733	-0.431	1.37	1.13	2.06	----	1.85	----	----	----	----	----	----	----	----	----	----	----	----	----	----
606.0621	1.557	-5.524	----	----	----	----	0.28	----	----	----	----	----	----	----	----	----	----	----	----	----	----
606.2846	2.176	-4.070	1.08	0.46	0.87	----	----	----	0.91	----	1.21	2.04	1.02	1.84	1.88	1.31	----	----	3.05	3.41	3.95
606.5482	2.608	-1.539	8.61	8.21	7.95	8.25	11.80	10.00	10.60	8.92	11.60	10.80	11.50	10.40	12.60	13.00	8.36	10.30	13.20	13.90	14.50
607.8491	4.795	-0.424	1.01	1.70	0.49	8.97	1.71	----	1.13	----	2.57	1.88	1.98	1.62	2.28	1.00	0.72	2.25	3.76	3.83	4.70
607.8999	4.652	-1.050	----	----	----	----	0.66	----	----	----	----	----	----	----	----	----	----	----	----	----	----
608.2708	2.223	-3.600	1.36	----	1.27	----	2.20	----	1.61	1.93	2.38	2.27	2.20	1.98	2.84	3.22	----	----	5.08	5.26	6.15
610.2173	4.835	-0.627	6.79	----	----	7.90	----	----	----	----	----	----	----	----	----	----	----	----	----	----	----
612.0244	0.915	-6.053	----	----	----	----	0.93	----	0.59	----	0.94	----	0.59	0.55	1.11	1.07	----	----	1.83	2.31	2.32
613.6993	2.198	-2.678	----	----	2.52	1.10	----	----	4.37	3.76	6.27	6.52	5.00	----	6.46	----	----	----	9.90	8.22	9.07
613.6615	2.453	-1.307	9.97	10.80	9.89	----	14.10	11.60	12.90	11.40	13.30	11.80	12.90	13.00	13.60	15.10	12.50	11.10	11.80	16.10	16.70

TABLE 2—*Continued*

Lambda	loggf	EP	M15 II75	M15 s6	M30 157	M30 sd	M55 283	M55 s76	M68 260	M68 53	N4833 13	N6144 152	N6397 603	N6397 669	N6397 302	N6397 331	N6397 468	N6397 428	N6752 29	N6752 36	N6752 284
613.7694	2.588	-1.507	9.86	9.51	8.86	9.77	12.50	10.30	11.40	10.50	12.80	12.10	12.00	11.30	12.80	15.40	9.07	6.59	13.60	15.20	15.80
615.1617	2.176	-3.350	3.12	1.41	1.50	2.34	4.04	1.85	2.91	2.75	4.36	4.13	4.07	3.28	5.00	5.69	1.58	----	7.08	7.52	7.48
617.3341	2.223	-2.990	4.86	3.13	4.74	3.24	----	----	5.22	4.96	----	----	----	----	----	----	----	----	----	8.52	8.94
618.0203	2.727	-2.710	----	----	----	----	4.70	1.68	----	----	----	----	----	----	----	----	----	----	----	----	----
620.0314	2.608	-2.420	3.21	2.33	4.87	3.01	5.46	3.78	4.87	4.06	6.70	6.13	----	5.31	6.60	4.02	3.01	----	8.67	9.54	9.23
621.3429	2.223	-2.456	5.60	5.20	5.39	5.58	8.99	6.47	7.76	6.62	8.93	8.62	8.58	8.17	9.16	11.90	5.18	8.85	9.65	10.80	11.90
621.9279	2.198	-2.641	7.38	5.27	6.08	5.51	9.85	6.52	8.31	7.56	9.46	8.45	9.18	9.02	9.98	11.70	6.21	8.00	10.70	12.50	12.30
622.9225	2.845	-2.900	----	----	----	1.42	1.53	----	0.85	0.79	3.44	3.24	2.37	2.04	2.23	2.76	----	----	3.25	3.63	5.10
623.2639	3.654	-1.271	4.30	0.92	2.53	1.26	4.22	3.19	3.24	2.74	3.97	5.05	4.00	3.61	4.04	3.76	1.42	4.43	6.05	7.46	----
623.8392	3.889	-2.630	----	----	0.76	0.74	1.68	----	1.25	----	----	----	0.68	1.04	1.92	----	----	----	2.28	2.93	2.89
624.0645	2.223	-3.360	1.77	----	----	----	4.50	----	----	1.77	----	----	----	----	----	----	----	----	----	----	----
624.7557	3.892	-2.329	1.38	----	----	----	----	----	----	----	----	----	----	----	----	----	----	----	----	----	----
625.2554	2.404	-1.699	----	----	----	----	12.40	10.60	----	----	----	----	----	----	----	----	----	----	----	----	----
626.5131	2.176	-2.252	4.81	6.03	6.15	4.43	9.04	6.80	9.39	7.13	10.30	7.83	9.16	8.16	9.91	12.30	6.06	2.97	11.30	11.80	12.10
627.0222	2.858	-2.640	----	1.13	1.62	3.02	2.54	1.91	1.80	1.37	3.50	2.63	2.82	2.60	3.16	3.90	1.10	----	6.01	5.82	6.91
627.1276	3.332	-2.880	----	1.21	----	----	0.23	----	0.88	----	0.79	----	1.69	0.92	0.53	1.31	----	----	1.61	1.68	2.63
628.0616	0.859	-4.390	4.69	2.51	5.00	7.33	10.90	6.83	9.63	3.48	9.23	11.80	8.97	8.60	10.60	13.40	7.62	5.83	11.60	13.60	11.50
629.7792	2.223	-2.780	4.52	4.88	4.49	4.06	7.50	4.88	6.64	5.70	7.62	7.54	7.58	6.20	7.86	10.20	5.07	6.13	9.73	10.70	10.60
630.1498	3.654	-0.745	3.95	2.31	----	3.83	7.51	5.70	----	----	----	----	----	----	----	----	----	----	----	----	----
630.2494	3.686	-1.203	3.34	1.97	----	2.29	4.94	3.58	3.61	2.61	2.47	----	4.11	4.14	5.14	5.12	2.08	----	6.30	8.35	8.00
631.1500	2.832	-3.160	----	1.15	1.34	----	----	----	0.42	0.70	----	0.37	----	----	----	----	----	----	4.31	2.99	3.20
632.2690	2.588	-2.304	----	----	----	----	6.41	4.71	----	----	----	----	----	----	----	----	----	----	----	----	----
633.5328	2.198	-2.114	8.33	8.42	7.33	8.86	10.90	8.67	10.60	8.90	11.70	10.30	10.00	9.29	11.00	13.10	6.86	6.38	11.60	12.80	12.90
633.6823	3.686	-1.016	2.41	0.52	3.17	4.74	5.82	4.67	5.61	3.81	7.05	7.28	5.38	5.40	6.33	6.99	2.90	4.95	8.60	8.83	9.06
634.4148	2.433	-2.920	2.83	3.08	2.08	1.82	4.92	3.26	3.69	3.24	3.87	3.57	4.29	3.72	5.57	6.33	2.52	----	7.34	7.99	8.90
635.3835	0.915	-4.846	----	----	----	----	----	----	0.39	----	----	----	----	----	----	----	----	----	0.98	----	----
635.5027	2.845	-2.350	3.14	----	2.03	1.41	4.81	3.43	3.30	3.26	6.39	5.19	4.31	3.52	5.50	5.56	3.40	----	7.55	7.83	8.56
636.9462	2.891	-4.253	2.98	0.64	----	2.03	0.99	----	----	1.24	----	----	----	----	----	----	----	----	----	----	----
638.0746	4.186	-1.330	----	----	1.16	1.08	----	----	1.17	----	----	----	----	----	2.74	----	----	----	4.11	3.75	2.16
639.3602	2.433	-1.599	----	----	----	----	12.80	11.20	----	----	----	----	----	----	----	----	----	----	----	----	----
640.8016	3.686	-1.048	2.94	0.37	2.68	3.48	5.35	3.83	4.42	3.17	5.00	6.69	5.31	4.33	5.36	6.40	2.76	----	----	8.14	8.66
641.1647	3.654	-0.788	4.87	4.40	4.43	5.29	8.20	6.84	6.63	5.18	8.77	8.44	7.69	7.60	8.28	9.26	5.58	5.59	10.60	10.50	11.00
641.9942	4.733	-0.230	0.91	0.73	1.57	1.30	1.96	1.84	1.30	0.91	2.51	3.84	2.18	2.35	2.31	4.31	1.06	----	4.55	5.22	6.04
642.1349	2.279	-1.954	9.52	8.68	8.23	8.90	11.80	9.28	10.90	9.96	12.80	11.20	11.50	10.80	11.30	13.10	9.06	11.50	13.00	14.40	13.70
643.0844	2.176	-2.016	9.97	8.71	8.86	10.10	13.00	10.80	11.80	10.50	13.50	12.10	12.10	11.90	13.10	14.60	8.63	----	14.10	15.10	15.90
645.6383	3.903	-2.075	----	4.29	1.69	3.56	3.86	----	2.51	1.46	----	----	----	2.51	2.51	----	----	----	3.00	4.74	4.02
647.5626	2.559	-2.870	1.30	1.68	1.91	3.27	4.25	2.30	2.46	3.21	4.53	4.88	4.34	2.88	4.46	----	----	----	6.63	6.84	8.09
648.1869	2.279	-2.990	3.35	----	----	1.75	5.86	3.91	4.70	3.74	6.41	5.82	5.39	4.47	5.82	7.16	4.02	3.44	8.40	9.68	9.29
648.3943	1.485	-5.228	----	----	----	3.79	0.43	----	----	----	----	----	----	----	----	----	----	----	----	----	----
649.4980	2.404	-1.331	2.40	12.90	10.50	12.40	14.10	10.90	15.40	13.70	15.30	15.00	13.70	13.20	15.20	15.90	11.00	11.60	16.00	17.20	17.90

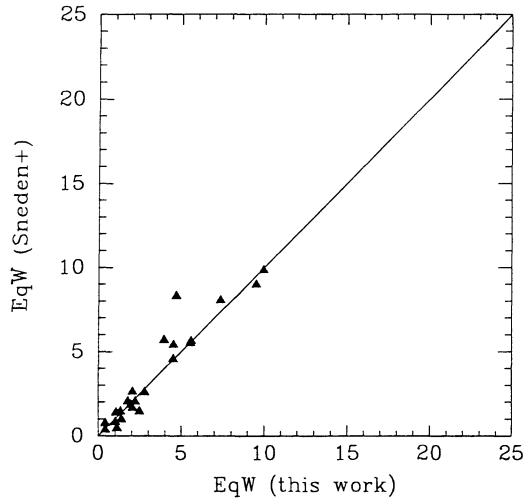

FIG. 2a

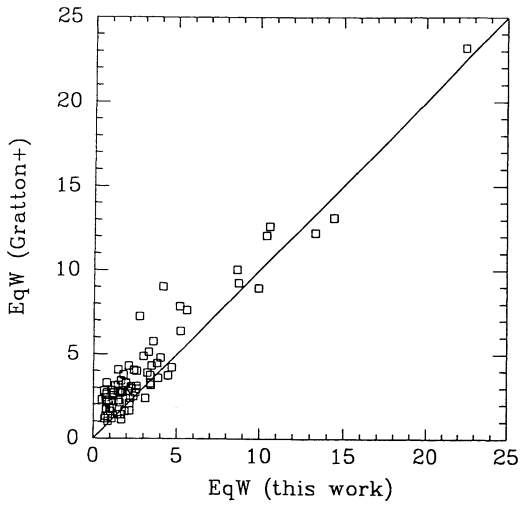

FIG. 2b

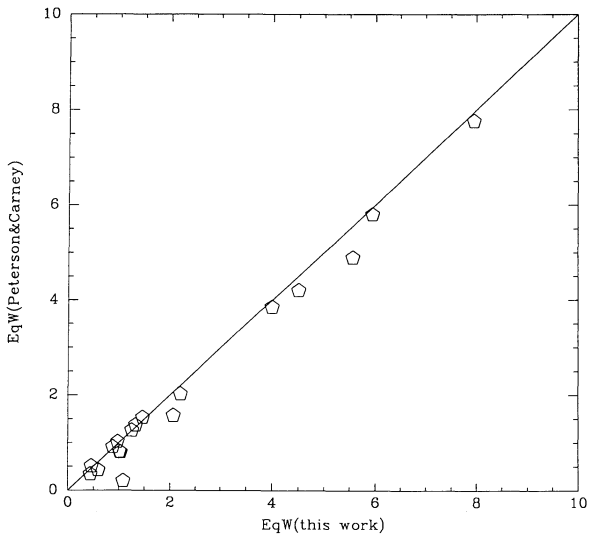

FIG. 2c

FIG. 2.—(*a*) Comparison of measured EW with SKPL for 22 lines in common in the stars HD 122563 and M15 star II-75. (*b*) Comparison with GO EW for 113 lines in common in the stars NGC 6397 star 669 and NGC 4590 star 260. (*c*) Comparison of measured EW with Peterson et al. (1990) for 17 lines in common in the star HD 122563.

especially for the weaker lines. These authors acknowledge there is a systematic difference between their EWs and those measured by Gratton (1988) using higher resolution and S/N, in the same sense and of about the same size as the difference we find. A similar effect is found by Zhao & Magain (1990). As discussed by GO, this would result in an overestimation of their metal abundance by about 0.15 dex. The larger EWs measured also require a larger microturbulent velocity to fit the models. Despite the small systematic difference between our measurements and those of GO, the abundances we derive are in excellent agreement with theirs, except for M68.

Given our S/N, we expect to be able to measure reliable EWs for lines as weak as ~ 0.5 nm. Lines stronger than ~ 14 nm are less sensitive to abundance. Therefore, we selected lines with $0.5 \leq \mathrm{EW} \leq 14$ nm.

3. MODELS

Recent improvements in model atmospheres and the addition of millions of new lines and improved opacities (Kurucz 1992a, b) allow extremely accurate determination of [Fe/H] from high-quality HDS data, especially for very metal-poor stars. Our method of analysis deserves some description here.

To obtain accurate abundances, one needs accurate knowledge of $T_{\rm eff}$, log g, and $V_{\rm tur}$ for a star. Instead of choosing the usual approach of getting the $T_{\rm eff}$ from published photometry, we took the photometric temperature only as an initial guess. Our procedure was to run different Kurucz models and determine $T_{\rm eff}$ from the dependence of [Fe/H] on excitation potential (EP) for the ensemble of lines, and then choose a $V_{\rm tur}$ from the dependence of [Fe/H] on EW. This procedure implies that the values of [Fe/H] derived here are independent of reddening uncertainties. The grid of models is shown in Figure 3. The steps of the grid were chosen every 0.5 dex in abundance, every 200 K in $T_{\rm eff}$, every 0.5 in log g, and every 0.5 km s^{-1} in $V_{\rm tur}$. A finer grid would not add much information and a coarser grid would yield large interpolation errors. Since we ran different models for each spectrum, the interdependence of all of the parameters is well determined. The final temperatures, then, were obtained solely from the spectra.

The relation

$$\log (g/g_0) = \log (M/M_0) + 4 \log (T/T_0) - \log (L/L_0)$$

was used to derive initial log g values, assuming $M = 0.8 M_0$, and L from the red giant (RG) sequence of Carbon et al. (1982). Gravities derived from IR photometry by Frogel, Persson, & Cohen (1983) are also available for about half of our sample. In all cases, the final value of log g was decided from the agreement between Fe I and Fe II line abundances.

Table 3 lists the results for all the runs of WIDTH. The final [Fe/H] values of the preferred fits are listed in Table 4, along with the adopted atmospheric parameters. There is a small range of parameter space that a good fit allows. Figure 4 illustrates how the final adopted parameters yield results with no systematic effects of the individual Fe abundances on λ, EW, or EP. We list the results of the individual models in Table 3 in case the reader prefers different values of $T_{\rm eff}$, log g, or $V_{\rm tur}$ for any star. These individual models also reflect the influence of variations of the input parameters on the derived abundance.

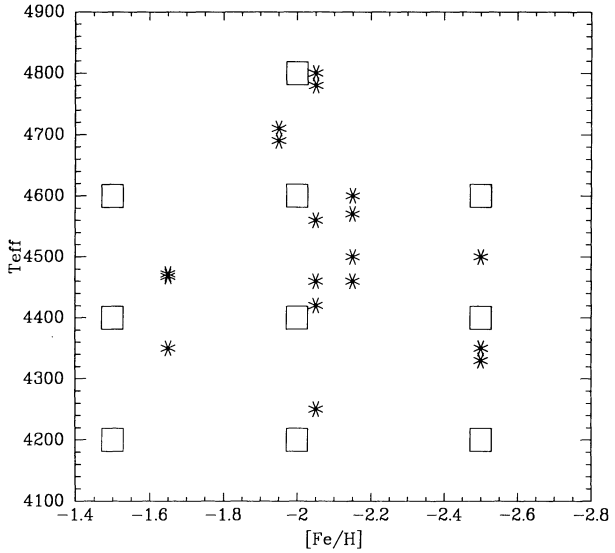

FIG. 3*a*

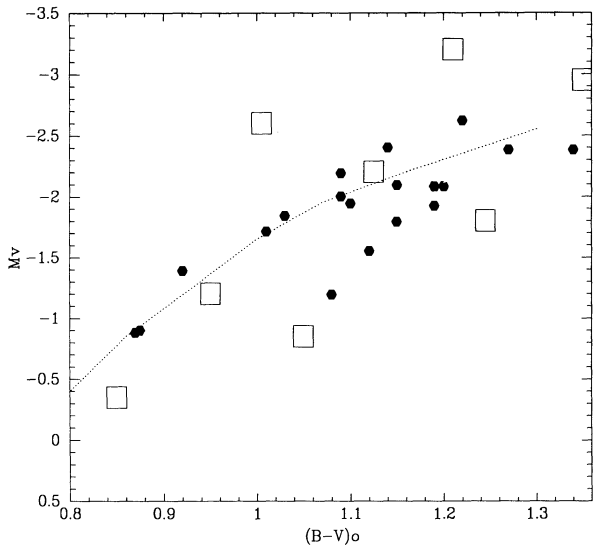

FIG. 3*b*

FIG. 3.—(*a*) Washington abundances vs. temperatures (*asterisks*) and the grid of models used in the spectroscopic abundance determinations (*squares*). (*b*) CMD for the program stars (*solid symbols*) with respect to the models (*big squares*). The dotted line is the position of the RGB of M92 from Carbon et al. (1982).

These effects are also discussed e.g. by GO and Peterson et al. (1990).

Table 5 summarizes the variations in [Fe/H] expected by changing the model input parameters by an amount larger than the expected error for a typical star. The largest uncertainty comes from the $T_{\rm eff}$. The final estimate of σ[Fe/H] is also listed in Table 5 and is $\sim$0.1 dex. This is the error associated with uncertainties in the model parameters. There is also the negligible internal error of $\leq$0.01 dex associated with the precision of the Fe abundance determination from the $\sim$50 lines. Finally, there is an additional $\sim$0.1 dex external error associated with the solar Fe abundance. Thus, we estimate the total uncertainty in our Fe abundances to be of the order of 0.15 dex.

After the line analysis was done, we generated synthetic spectra for all of our stars using as input parameters the final values from the line analysis. There is in all cases excellent agreement between the abundances derived from the two techniques, lending confidence to the abundances listed in Table 4. Model atmospheres for very metal-poor stars are more accurate at reproducing the observations than for more metal-rich stars, mainly because they are simpler, with fewer lines and therefore less missing opacity, and the temperature is more easily estimated. The synthetic spectra reproduce the observations for the highest S/N spectra in great detail, and the small departures in the lower S/N spectra can be attributed solely to Poisson statistics.

4. COMPARISON TO PREVIOUS RESULTS

4.1. *Comparison of Individual Stars*

The final Fe abundances we derive are presented in Table 6, along with other HDS values and those from Z85 and GMC for comparison. Note that all of the HDS values have been converted to our assumed solar scale, with Fe = 7.5. We first discuss individual star abundances in common with other HDS studies and then compare cluster mean values to these other determinations. Comparison with a host of other abundance determinations for these globular clusters could be made but would be too lengthy, so we will restrict our discussion to a comparison with our previous work on Washington photometry (GMC), with Z85, and with the other HDS determinations.

Four of our stars have previous HDS abundances: M68 star 260, with [Fe/H] = −1.94 from GO versus −2.12 (this work), NGC 6397 star 669, with [Fe/H] = −1.78 from GO versus −1.99 (this work), NGC 6397 star 428, with [Fe/H] = −1.90 from GO versus −1.99 (this work), the M15 star II-75 with [Fe/H] = −2.26 (mean of their two values obtained assuming different $T_{\rm eff}$) from SKPL versus −2.27 (this work). Clearly, the differences are within the errors, and the agreement is excellent.

4.2. *Comparison of Individual Clusters*

Our mean cluster abundance for M68 from two stars is -2.17 ± 0.05 (standard error of the mean). This cluster has HDS abundances from GO, who find a mean of [Fe/H] = −1.9 from two stars. This is by far the largest discrepancy between our abundances and other HDS cluster studies. A significantly lower abundance than that of GO is indicated by both Z85 and GMC. Indeed, M68 is one of the clusters suspected by GMC of being substantially more metal-poor than given by Z85. Our present value is intermediate but closer to the Z85 value.

M68 has gained additional notoriety recently with the publication of cluster ages based on ΔV(HB − TO) by Chaboyer, Sarajedini, & Demarque (1992), in which they find that this cluster could be younger than the canonical metal-poor globulars M15, M92, and M30. Support for a younger age for M68 also comes from Figures 36 of Stetson & Harris (1988), where M68 appears to have a brighter turnoff than M30 or M92. In contrast, VandenBerg, Bolte, & Stetson (1990) find no spread in ages among these most metal poor globulars, including M68. However, the *absolute* age determined for M68 will *increase* if our abundances are assumed. McClure et al. (1987) derived an age of 14 Gyr, assuming [Fe/H] = −2 and [O/Fe] = +0.7. Holding the other parameters (Y, reddening, and distance) fixed, the metallicity and O abundance (Minniti et al. 1993a) we derive would yield an age $\sim$2 Gyr older.

TABLE 3

RESULTS FROM WIDTH FOR METAL-POOR GLOBULAR CLUSTER STARS

M/NGC	STAR	NUMBER OF LINES Fe I	NUMBER OF LINES Fe II	Model	T	log g	v_{tur}	SLOPE EP	SLOPE EW	Fe I	Fe II
M68	53	54	3	−2.5	4200	1.0	2.0	0.068	−0.013	−7.01	−6.56
				−2.0	4400	1.0	2.0	0.006	−0.002	−6.81	−6.55
				−2.5	4400	1.0	2.0	−0.010	0.006	−6.73	−6.65
				−2.5	4600	1.5	2.5	−0.046	−0.002	−6.55	−6.50
M68	260	61	4	−2.5	4200	1.0	2.0	0.076	0.001	−6.86	−6.59
				−2.0	4400	1.0	2.0	0.013	0.009	−6.65	−6.61
				−2.5	4400	1.0	2.0	−0.003	0.015	−6.57	−6.70
				−2.5	4600	1.5	2.5	−0.039	0.006	−6.40	−6.56
M30	D	50	5	−2.5	4400	1.0	2.0	0.073	0.045	−6.69	−6.60
				−2.5	4600	1.5	2.0	0.008	0.057	−6.52	−6.51
				−2.0	4600	1.5	2.5	0.031	0.032	−6.58	−6.13
				−2.0	4400	1.0	2.0	0.085	0.039	−6.77	−6.24
				−2.5	4400	1.5	2.0	0.078	0.043	−6.73	−6.12
M30	157	47	4	−2.5	4600	1.5	2.0	0.003	−0.016	−6.59	−6.74
				−2.0	4600	1.5	2.0	0.013	−0.022	−6.66	−6.70
				−2.0	4400	1.0	1.5	0.048	−0.009	−6.83	−6.81
M15	s6	46	5	−2.5	4400	1.0	2.0	0.036	0.010	−6.89	−6.60
				−2.5	4600	1.5	2.5	0.002	0.002	−6.71	−6.42
				−2.5	4200	1.0	2.0	0.115	−0.006	−7.17	−6.44
				−2.5	4400	1.5	2.0	0.045	0.007	−6.92	−6.34
M15	II-75	41	7	−2.5	4400	1.0	2.0	0.008	−0.009	−6.77	−6.77
				−2.5	4600	1.5	2.0	−0.058	0.008	−6.52	−6.80
				−2.0	4600	1.5	2.0	−0.045	0.001	−6.60	−6.20
				−2.0	4200	1.0	1.5	0.056	0.002	−7.05	−6.15
				−2.5	4200	1.0	1.5	0.052	0.004	−7.00	−6.24
M55	283	66	1	−2.5	4400	1.0	2.0	−0.060	0.010	−6.38	−6.57
				−2.5	4600	1.5	2.5	−0.094	0.001	−6.22	−6.25
				−2.0	4600	1.5	2.5	−0.078	−0.005	−6.30	−6.18
				−2.0	4400	1.0	2.0	−0.044	0.005	−6.47	−6.32
				−2.5	4400	1.5	2.0	−0.056	0.008	−6.42	−6.21
M55	76	42	0	−2.0	4400	1.5	2.0	...	...	−6.80	...
				−2.5	4600	1.5	2.0	−0.027	0.013	−6.42	...
				−2.0	4600	1.5	2.0	−0.013	0.006	−6.50	...
				−2.0	4400	1.0	2.0	0.059	−0.010	−6.76	...
N6144	15	50	2	−2.0	4400	1.0	1.5	0.027	0.013	−6.25	−6.02
				−2.0	4600	1.5	2.0	0.002	−0.004	−6.13	−6.02
				−2.5	4600	1.5	2.0	−0.017	0.004	−6.04	−6.08
				−2.0	4200	1.0	1.5	0.094	0.002	−6.51	−5.91
				−2.5	4200	1.0	1.5	0.091	0.003	−6.46	−6.03
				−1.5	4400	1.0	2.0	0.028	−0.015	−6.15	−6.02
N4833	13	52	1	−2.5	4400	1.0	2.0	0.031	0.021	−6.27	−6.31
				−2.5	4600	1.5	2.0	−0.007	0.009	−6.13	−6.17
				−2.0	4600	1.5	2.5	0.007	0.004	−6.21	−6.10
				−2.0	4400	1.0	2.0	0.047	0.015	−6.36	−6.21
				−1.5	4400	1.0	2.0	0.069	0.006	−6.39	−6.22
N6397	302	55	4	−2.0	4400	1.0	2.0	−0.027	−0.005	−6.44	−6.47
				−2.5	4600	1.5	2.5	−0.074	−0.008	−6.20	−6.42
				−2.0	4600	1.5	2.0	−0.104	0.011	−6.19	−6.39
				−2.0	4200	1.0	2.0	0.041	−0.016	−6.70	−6.33
N6397	603	53	3	−2.5	4400	1.0	2.0	−0.002	−0.006	−6.44	−6.61
				−2.5	4600	1.5	2.0	−0.077	−0.010	−6.19	−6.39
				−2.0	4600	1.5	2.0	−0.061	0.063	−6.28	−6.36
				−2.0	4200	1.0	1.5	0.033	0.010	−6.68	−6.30
N6397	669	50	4	−2.0	4400	1.0	2.0	−0.006	−0.014	−6.59	−6.51
				−2.0	4600	1.5	2.0	−0.078	−0.001	−6.34	−6.40
				−2.0	4200	1.0	1.5	0.018	0.008	−6.75	−6.37
N6397	a331	51	4	−2.0	4400	1.0	2.5	−0.047	−0.001	−6.40	−6.50
				−2.0	4200	1.0	2.0	−0.030	0.012	−6.56	−6.33
				−2.0	4200	0.5	2.0	−0.020	0.010	−6.55	−6.55
N6397	428	19	1	−2.0	4800	1.5	2.5	−0.036	0.021	−6.40	−6.40
				−2.0	4600	1.5	2.0	−0.006	0.035	−6.59	−6.29

TABLE 3—*Continued*

M/NGC	Star	Number of Lines: Fe I	Fe II	Model	T	log g	v_{tur}	Slope EP	Slope EW	Fe I	Fe II
N6397	468	41	2	−2.0	4800	1.5	2.5	−0.085	0.022	−6.45	−6.43
				−2.0	4600	1.5	2.0	−0.057	0.028	−6.65	−6.33
N6752	284	56	4	−2.0	4400	1.0	2.0	−0.001	−0.010	−5.98	−6.15
				−2.5	4600	1.5	2.0	−0.102	0.011	−5.62	−6.12
				−2.0	4600	1.5	2.0	−0.082	0.004	−5.72	−6.10
				−2.0	4200	1.0	1.5	0.017	0.010	−6.05	−6.00
				−1.5	4400	1.0	2.0	0.027	−0.020	−6.03	−6.16
N6752	36	60	4	−2.0	4400	1.0	2.0	0.015	−0.014	−6.01	−6.11
				−2.5	4600	1.5	2.0	−0.088	0.009	−5.65	−6.08
				−2.0	4600	1.5	2.0	−0.066	0.001	−5.75	−6.07
				−2.0	4200	1.0	1.5	0.032	0.006	−6.09	−5.96
				−1.5	4400	1.0	2.0	0.044	−0.025	−6.05	−6.12
N6752	29	50	4	−2.0	4400	1.0	2.0	0.089	−0.020	−6.12	−6.22
				−2.0	4600	1.5	2.0	0.012	−0.006	−5.86	−6.12
				−2.0	4200	1.0	1.5	0.012	0.004	−6.22	−5.98
				−1.5	4400	1.0	1.5	0.113	−0.031	−6.16	−6.23

Our single star in NGC 4833 yields a Fe abundance of −1.71, in excellent agreement with the GO result of −1.74 from two stars, and much larger than the GMC value. GMC discussed the large range of $E(B-V)$ values reported for this cluster, and its possible influence on the very low [Fe/H] derived from Washington photometry. Indeed, Minniti, Coyne, & Claria (1992) found reddening variations across the face of the cluster from polarimetric observations of individual red giants. Thus, it is very likely that most or all of the giants observed by GMC have reddenings substantially larger than the mean value they assumed.

NGC 6144 is also a very reddened cluster, with no high-dispersion chemical compositions published, although unpublished Washington photometry suggests that it is a very metal-poor cluster. Our single star gives [Fe/H] = −1.59, in reasonable agreement with the Z85 abundance. Further HDS of the giants in this cluster are desirable, as is a more detailed reddening and CMD investigation.

NGC 6397 is the closest very metal-poor globular, at a distance of 2.2 kpc. In spite of lying ∼2° away from the star-forming complex ρ Oph, its reddening is moderately low and uniform (Minniti et al. 1992). HDS abundances are given by GO for three red giant stars (mean [Fe/H] = −1.88), and by Lambert, McWilliam, & Smith (1992) for one horizontal-branch star ([Fe/H] = −1.96). These metallicities are in excellent agreement with the presnt value of −1.99 ± 0.01, as are the Z85 and Washington values. Note that the total spread in our six stars is only 0.01 dex, due to the high S/N achieved in these particular spectra.

NGC 6752 is one of the brightest and closest clusters, and an obvious target for high-dispersion studies. GO obtained [Fe/H] = −1.53 from three stars, within 0.05 dex of our value. Indeed, all of the values in Table 6 are very close. Note that our sample of three giants shows a spread of only 0.04 dex.

M55 is another bright, nearby cluster but as yet has not been subject to HDS (note that the previous work of Pilachowski et

TABLE 4

Final Iron Abundances

M/NGC	Star	T_{eff}	log g	V_{tur}	[Fe I/H]	[Fe II/H]	Cluster Mean[a]
M68	53	4400	1.0	2.0	−2.27	−2.10	
M68	260	4400	1.0	2.0	−2.11	−2.14	−2.17
M30	D	4600	1.5	2.0	−2.02	−2.02	
M30	157	4600	1.5	2.0	−2.16	−2.23	−2.10
M15	II-75	4400	1.0	2.0	−2.27	−2.27	
M15	s6	4500	1.3	2.0	−2.28	−2.00	−2.23
M55	283	4400	1.0	2.0	−1.97	−1.82	
M55	76	4400	1.0	2.0	−2.00	...	−1.96
N6144	152	4600	1.5	2.0	−1.63	−1.52	−1.59
N4833	13	4500	1.3	2.0	−1.74	−1.66	−1.71
N6397	302	4400	1.0	2.0	−1.94	−1.97	
N6397	603	4400	1.0	2.0	−1.95	−2.00	
N6397	669	4400	1.0	2.0	−2.00	−1.98	
N6397	a331	4200	0.5	2.0	−2.00	−1.98	
N6397	428	4600	1.5	2.0	−2.00	−1.98	
N6397	468	4600	1.5	2.0	−2.00	−1.98	−1.99
N6752	284	4400	1.0	2.0	−1.48	−1.65	
N6752	36	4400	1.0	2.0	−1.51	−1.61	
N6752	29	4400	1.0	2.0	−1.61	−1.72	−1.58

[a] Solar Fe = 7.50 adopted (Holweger et al. 1990, 1991).

TABLE 5

Errors in the Abundance for NGC 6397 Star 302

A. Best Model: AM = −2.0; T = 4400 K; log g = 1.0; V_t = 2.0

ΔAM = −0.5	Δ[Fe/H] = −0.02
Δ log g = −0.5	Δ[Fe/H] = −0.10
Δ log g = +0.5	Δ[Fe/H] = +0.09
ΔT = +100.....	Δ[Fe/H] = +0.05
ΔT = −100.....	Δ[Fe/H] = −0.03
ΔV_t = +0.5	Δ[Fe/H] = −0.08
ΔV_t = −0.5	Δ[Fe/H] = +0.11

B. Probable Uncertainties in the Parameters Chosen for Best Model

σAM = ±0.2
σlog g = ±0.2
σT = ±75
σV_t = ±0.25

C. Summary: Total Uncertainty

σ[Fe/H] = 0.09

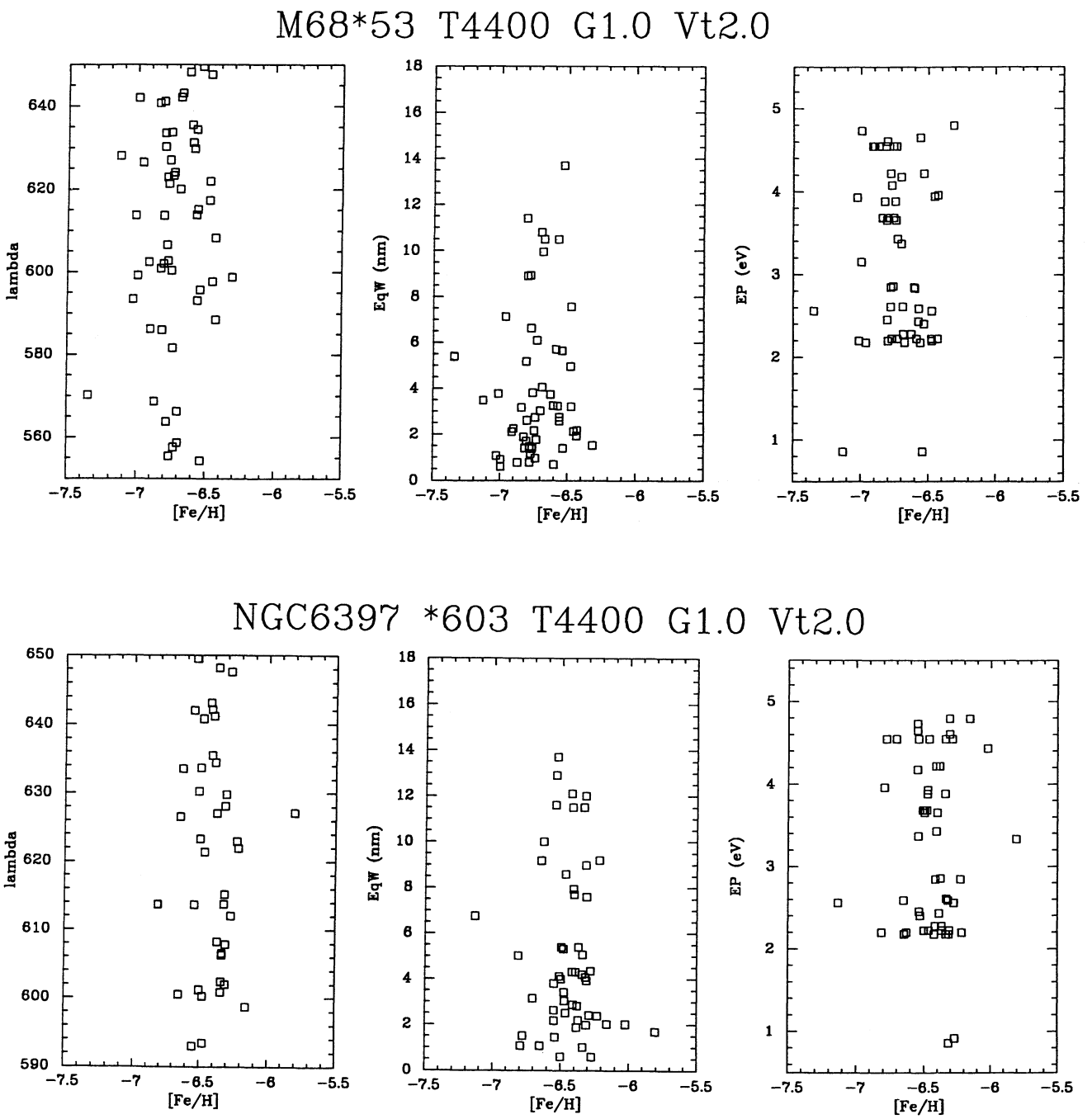

FIG. 4.—[Fe/H] line abundance vs. wavelength, equivalent width, and excitation potential for the stars NGC 6397 star 603 (S/N = 90), M68 star 53 (S/N = 65), and M55 star 283 (S/N = 40). Note the lack of any trend, indicating appropriate choices for the model parameters.

al. (1984) and Caldwell & Dickens (1988) based on echelle spectra are of insufficient quality to qualify as HDS). Both the Zinn and Washington abundances are in very good accord with our present value of -1.96 ± 0.04 from two stars, whose individual abundances lie within 0.08 dex of each other.

M15 has long been regarded as a classical metal-poor cluster and as such is the basis for several metal abundance calibrations. However, the only HDS determination of metal abundance is that of SKPL. They obtain [Fe/H] = −2.30 based on three stars, although as they point out, this value would be 0.1 dex higher should they have adopted the distance modulus and reddening from Trefzger et al. (1983). Our value is -2.23 ± 0.04, with two stars falling within 0.08 dex. Again, the various independent determinations in Table 6 are in excellent agreement.

There is no high-dispersion abundance determined for M30, despite its proximity. Nonetheless, M30 is used as a standard metal-poor cluster for a variety of studies because its giants are

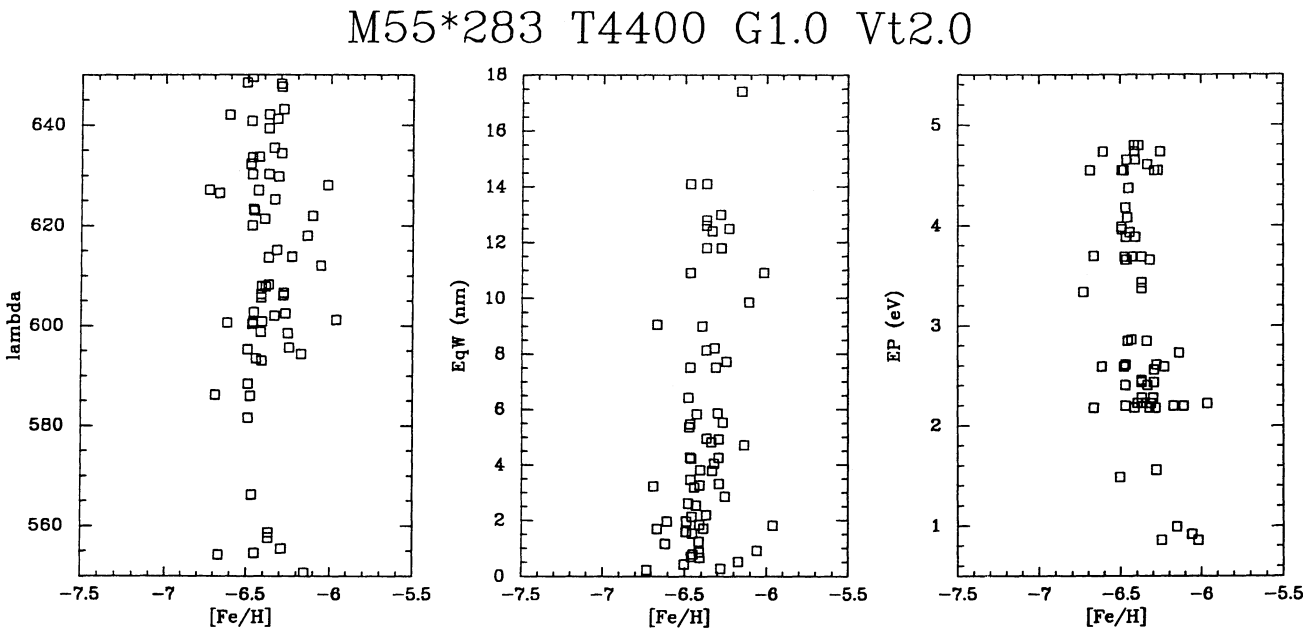

FIG. 4—*Continued*

bright. Our two stars have metallicities that differ by 0.16 dex, for a mean of -2.11 ± 0.08. Both the Z85 and Washington abundances are in excellent agreement.

5. DISCUSSION

5.1. *Calibration of the Metal-poor End of the Abundance Scale*

Leep, Oke, & Wallerstein (1987) and SKPL argue that the metal-poor end of the globular cluster abundance scale is uncertain to ~ 0.2 dex, due to different random and systematic effects ($T_{\rm eff}$ vs. photometric colors, solar composition, model atmosphere parameters, etc.). With the present results in hand, which greatly increase the number of metal-poor globulars with at least two independent HDS studies, a closer look at this situation is warranted.

Five of our eight clusters have had previous HDS results. Four of these (M68, NGC 4833, NGC 6397, and NGC 6752) are in common with GO, while the fifth (M15) was studied by SKPL. To summarize the above comparisons discussed individually, our value for M15 is 0.05 dex higher than that of SKPL (when placed on our solar Fe scale), while our values are 0.09 ± 0.12 dex lower than those of GO. The mean difference for all five clusters is 0.06 ± 0.12. These clusters range over almost a factor of 10 in metallicity.

These small differences are well within the respective errors and encourage us to suggest that the low end of the abundance scale for globulars is now tied in to ~ 0.1 dex by HDS. This is as long as the same solar composition is assumed.

Since Galactic globulars are used in calibrating many photometric and spectroscopic indices for a variety of Galactic and extragalactic research, it is important to derive the best possible calibration of their abundances. Thus, in the fifth column of Table 6 we list our final preferred values to define the [Fe/H] scale at the metal-poor end of the globular cluster system ([Fe/H] ≤ -1.5). We have added independent values for other clusters with HDS. It is this fifth column that should be used for calibration purposes at the low-metallicity end. The [Fe/H] values listed in Table 6 are the mean of different HDS studies, weighted by the number of stars observed. The results of Table 6 were computed assuming a solar Fe abundance of 7.50 recommended by Holweger et al. (1990, 1991), and they might be shifted if a different value of $Fe_{\odot}$ is determined to be more accurate, depending on whether or not the original value derived from solar or laboratory *gf*-values.

We can now use our newly defined HDS Fe abundance scale for metal-poor globular clusters to investigate the Z85 and Washington scales. These respective values for the clusters in Table 6 are given in columns (6) and (7). The Washington values are from GMC, Geisler, Claria, & Minniti (1991), and some unpublished data.

Figure 5 shows that the Z85 abundances correlated very well with our adopted HDS scale. This is not completely surprising, given that a number of the values are derived from GO, who showed a similarly good correlation between their results and those of Zinn (1980), on which many of the Z85 values are

TABLE 6

COMPILATION OF [Fe/H] VALUES FOR METAL-POOR GLOBULAR CLUSTERS WITH HDS

NGC (1)	This Paper (2)	Other (3)	Source[a] (4)	HDS (5)	Z85 (6)	Washington (7)
1904....	...	−1.46	1	−1.46	−1.68	−1.71
2298....	...	−1.89	2	−1.89	−1.81	−2.50
4590....	−2.17	−1.92	3	−2.05	−2.09	−2.50
4833....	−1.71	−1.74	3	−1.73	−1.86	−2.50
5272....	...	−1.45	4	−1.45	−1.66	−1.39
5897....	...	−1.84	3	−1.84	−1.68	−2.50
6144....	−1.59	...	—	−1.59	−1.75	...
6205....	...	−1.49	4	−1.49	−1.65	−1.53
6341....	...	−2.23	5, 6	−2.23	−2.24	−2.42
6397....	−1.99	−1.88	3	−1.93	−1.91	−2.05
6752....	−1.57	−1.53	3	−1.55	−1.54	−1.65
6809....	−1.95	...	—	−1.95	−1.82	−1.95
7078....	−2.23	−2.28	5	−2.26	−2.15	−2.15
7099....	−2.11	...	—	−2.11	−2.13	−2.15

SOURCES.—(1) Francois 1991; (2) McWilliam et al. 1992; (3) GO; (4) Kraft et al. 1992; (5) SKPL; (6) Peterson et al. 1990.

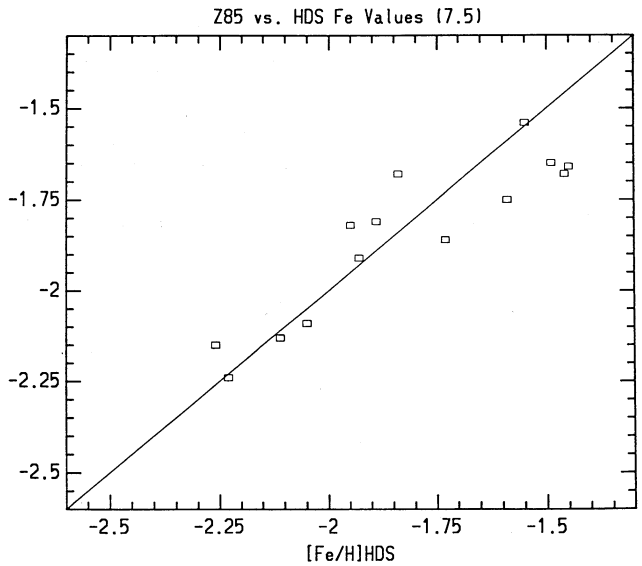

FIG. 5.—Metal abundances from Zinn (1985) vs. those from our new HDS-based scale for globular clusters with [Fe/H] < -1.5. Note the excellent correlation and small differences.

based. For the sample of 14 clusters, all with blue horizontal branches, the Z85 values are only 0.01 dex more metal-poor in the mean, with a standard deviation of 0.13 dex. We note that the Z85 results are largely reddening-independent. Our results corroborate a number of other studies which demonstrate that the Z85 scale is on firm footing.

The comparison with the Washington scale is not as good, as shown in Figure 6. Although most of the clusters lie near the line of equality, four of them fall far below the line. Of these, two (NGC 2298 and NGC 4833) have very uncertain reddenings. As discussed by GMC, the Washington abundances for cool, metal-poor giants are very sensitive to reddening. The reddenings for the other two disparate clusters,

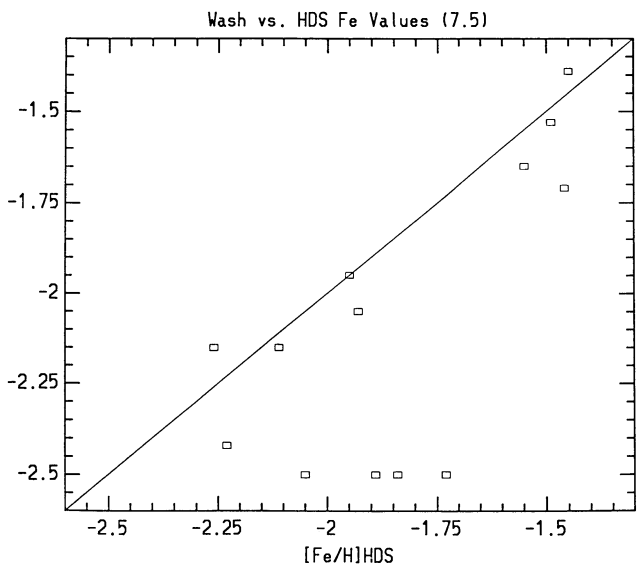

FIG. 6.—Metal abundances from Washington photometry vs. those from our new HDS-based scale for globular clusters with [Fe/H] < -1.5. The scatter is larger than in Fig. 5, and there are several clusters with anomalously low Washington abundances, probably due to reddening errors.

M68 and NGC 5897, are small and known to higher accuracy, so this error source is unlikely to account for the entire discrepancy. However, the problem does not appear to be due to a difference in scales, as the Washington abundances for many of the most metal-poor clusters are in very good agreement with the HDS results. Note that the HDS value for M68 in Figure 6 is the mean of two studies and that our value is much lower than that of GO. Discarding NGC 2298 and NGC 4833, we find that the comparison of the Washington and HDS values has a standard deviation of 0.23 dex. This error is about what one would expect from the decreased metallicity sensitivity of the Washington system at low abundances. Including the two discrepant clusters, the difference between Washington and HDS rises to 0.23 ± 0.30 dex.

5.2. *Globular Cluster versus Field Halo Stars*

Different systematics affect the abundance determinations in field halo stars and globular cluster giants. For example, the halo stars tend to be closer and brighter, making it possible to achieve much higher signal-to-noise ratio spectra, while in globular clusters the determination of $T_{\rm eff}$, log g, and $E(B-V)$ is more reliable.

Even though the metallicity distribution functions of field halo stars and globular clusters peak at the same value, there is a dramatic lack of very metal-poor clusters (Laird et al. 1988; Ryan & Norris 1991). Indeed, the significance of this difference now exceeds 99% from the results of the latest compilation of subdwarfs (Laird 1993). This difference is one of the primordial signatures of halo formation that still remains to be explained. The suggestion by GMC that there may be a substantially larger number of metal-poor clusters than previously believed is not borne out by the present analysis. However, this does not mean that the field halo stars and globulars come from two different parent populations. This is because (1) the globular cluster population has a limited size, and statistical noise could bias the interpretations (although the latest results by Laird seem to rule out this possibility); and (2) the survival of globulars is dictated by external factors (Fall & Rees 1984; Caputo & Castellani 1984), and a significant fraction of globulars may well have been disrupted during a Hubble time. These disrupted globulars supply the halo with stars. Of course, not all halo stars necessarily come from disrupted globulars. However, there is growing evidence for comoving groups of halo stars (Dionidis & Beers 1989; Eggen & Iben 1990; Schuster & Nissen 1992; Arnold & Gilmore 1992; Majewski 1992). In particular, a three-dimensional knowledge of globular cluster orbits (Cudworth & Hanson 1993) would contribute much to this scenario by confirming the Frenk & White (1980) results on the shapes of the cluster orbits, and determining the systematics of the disruption processes which are expected to vary according to the orbital parameters (Chernoff & Shapiro 1987).

5.3. *Self-Enrichment*

Morgan & Lake (1989) and Brown, Burkert, & Truran (1991) have recently discussed the self-enrichment of globular clusters and its implications for mass and metallicity limits. They have argued that it is likely that every globular cluster has experienced at least one supernova (SN) explosion during its formation and thus self-enrichment is likely if the cluster is sufficiently massive to retain the remnant. The metallicity range observed among halo globulars can be well reproduced by self-enrichment of initially zero metallicity protoclusters

(Brown et al. 1991), as can their mass range (Morgan & Lake 1989).

The most interesting clusters in the self-enrichment scenario are the ones that are the most metal poor and at the same time least massive, because there should be a lower mass limit below which a protoglobular cluster is disrupted after only a single SN II explosion. Theoretically, this limit depends on the details of the cooling curve adopted (Morgan & Lake 1989). We can address this issue observationally.

We will assume that all of the very metal poor globulars ([Fe/H] ≤ -1.75) are only self-enriched. We can then plot cluster mass versus number of SNs, or equivalently, metal abundance. Figure 7 shows this plot, where the masses are from Chernoff & Djorgovski (1989) and the metallicities are our HDS values or those of Z85. The metal production of a typical SN II like SN 1987A (Arnett et al. 1989) distributed through the present mass of a globular cluster would give a metal abundance denoted by the line.

According to Figure 7, the globulars of lower mass and metallicity could have been self-enriched by only about five to 10 SN II's. On these grounds, we do not expect to find globulars as metal-poor as -2.5 dex and less massive than $\sim 10^{4.5}$ $M_{\odot}$, and indeed none exist. This agrees with the calculations of Morgan & Lake (1989) and Brown et al. (1991).

These same clusters might also be expected to exhibit statistical fluctuations in the abundances of different elements from star to star due to the different masses of the (few) SN II progenitors. An excellent cluster for such a search is NGC 6397, which lies in a position (-1.93, 4.77) suggesting self-enrichment by less than 10 SNs like SN 1987A, and is also very nearby, allowing high-resolution observations of a number of giants.

However, a strong constraint on self-enrichment is imposed by the very small upper limits on internal metal abundance spreads deduced from modern CCD CMD and HDS studies. For example, Da Costa & Armandroff (1990) find that the metal abundance spread in NGC 6397 must be ≤ 0.06 dex from the tightness of the giant branch in their $V-I$ photometry. This implies, if self-enrichment is responsible for the metal production, that the explosions were very isotropic and that mixing of their ejecta was very efficient. However, since light elements such as O and Mg are produced by more massive SNs, one might expect to see internal variations in these elements and not Fe. Such a study is under way (Minniti et al. 1993b).

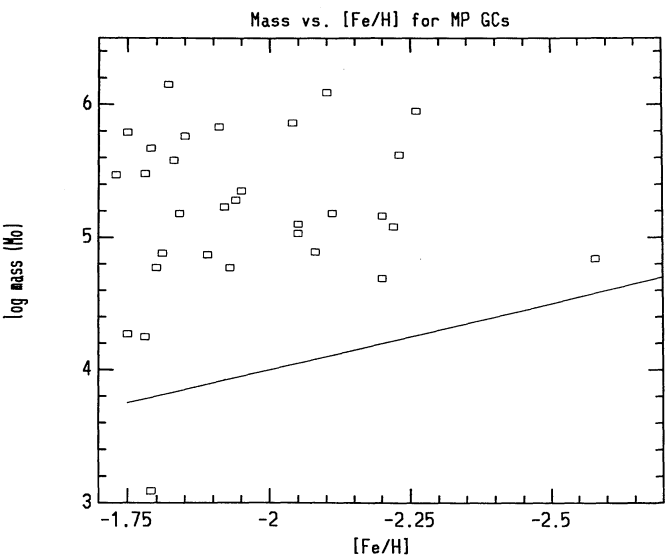

FIG. 7.—Log of the mass of metal-poor globular clusters vs. metallicity. The line is derived by uniformly distributing the metal production of SN 1987A throughout a cluster and provides a lower boundary to the observed distribution, suggesting self-enrichment by SNs may play an important role in the chemical evolution of globular clusters.

Protoglobular clusters that lie below the line in Figure 7 presumably would have been disrupted by the explosion(s), and the stars formed in the debris would be identified now as field halo stars. The lone cluster in this region is Pal 13, which is an order of magnitude less massive than any other cluster in the sample. Perhaps it formed later, from already enriched material, and did not have to survive a SN II explosion. It is important to remark that the position of the line corresponds to an ~ 25 $M_{\odot}$ SN II, and that progenitors of different masses would produce different amounts of heavy elements (e.g., Nomoto et al. 1992). Indeed, the apparent consistency between the clusters and the SN line does not necessarily imply that the clusters did in fact self-enrich. Nonetheless, the general agreement between the boundary set by the line and the observed cluster distribution is intriguing and suggests that detailed spectroscopic abundances for many elements and stars in such clusters might lead us to a better understanding of the number, masses, and type of primordial SNs that may have enriched the most metal poor globular clusters.

6. SUMMARY

We have obtained high-resolution, high S/N CCD spectra for 16 giants in eight metal-poor Galactic globular clusters. Fe abundances accurate to 0.15 dex (including internal errors and uncertainties in the model atmosphere parameters and solar Fe abundance) have been determined by means of a fully consistent set of model atmospheres and spectrum synthesis techniques. The agreement with previous high-quality metallicity determinations is excellent, from which we conclude that the low end of the globular cluster metallicity scale is secured to ~ 0.1 dex. We present a metallicity scale for metal-poor clusters based on HDS that should prove useful for calibrating a wide variety of photometric and low-resolution spectroscopic metallicity indicators. We compare this metallicity scale to that of Z85 and Washington photometry. The Zinn scale agrees very well with the HDS scale, with a negligible mean offset and a typical error of only 0.13 dex. The offset for the Washington abundances is larger, mostly due to a few clusters that are most likely affected by reddening. The large reddening sensitivity and reduced metallicity sensitivity of this system for cool, metal-poor giants is responsible for the larger errors, ~ 0.23 dex. However, we find that M68, like NGC 2298, is more metal-poor than the Z85 value, as suggested by the Washington photometry of GMC.

The accurate determination of [Fe/H] for a large sample of metal-poor globulars is an important datum necessary in deriving ages from a variety of fitting techniques. The second paper in this series will present α element abundances, including O, and allow us to address absolute age determinations extensively. Finally, the metallicity of many metal-poor clusters may be explained by the self-enrichment of a zero metallicity protocluster due to the explosion of a small number of Type II SNs.

We would especially like to thank Bob Kurucz and Cristina Dalle Ore for assistance in computing the model atmospheres. We are grateful to Mario Hamuy and Lisa Wells at CTIO, and Nigel Sharp and Jeannette Barnes at KPNO, for help with the reductions. Also thanks to Hernan Tirado and all the CTIO people for help on the mountain. D. M. acknowledges partial support from E. Olszewski (NSF grant AST86-11405), and J. Liebert (NASA grant NAG 5-1144). J. J. C. is supported by Conicet and Conicor of Argentina.

REFERENCES

Alcaino, G. 1971, A&A, 13, 287
———. 1972, A&A, 16, 220
———. 1975, A&AS, 22, 193
———. 1977a, A&AS, 29, 9
———. 1977b, A&AS, 29, 397
———. 1980, A&AS, 39, 315
Alcaino, G., & Liller, W. 1980, AJ, 85, 1330
Anders, E., & Grevesse, N. 1989, Geochim. Cosmochim. Acta, 53, 197
Arnett, W. D., Bahcall, J. N., Kirshner, R. P., & Woosley, S. E. 1989, ARA&A, 27, 629
Arnold, R., & Gilmore, G. 1992, MNRAS, 257, 225
Armandroff, T. E. 1989, AJ, 97, 375
Armandroff, T. E., Da Costa, G. S., & Zinn, R. 1992, AJ, 104, 164
Brown, J. H., Burkert, A., & Truran, J. W. 1991, ApJ, 376, 115
Caldwell, S. P., & Dickens, R. J. 1988, MNRAS, 234, 87
Cannon, R. D. 1974, MNRAS, 167, 551
Caputo, F., & Castellani, V. 1984, MNRAS, 207, 185
Carbon, D. F., Langer, G. E., Butler, D., Kraft, R. P., Suntzeff, N. B., Kemper, E., Trefzger, C. F., & Romanishin, W. 1982, ApJS, 49, 207
Chaboyer, B., Sarajedini, A., & Demarque, P. 1992, ApJ, 394, 515
Chernoff, D. F., & Djorgovski, S. 1989, AJ, 339, 904
Chernoff, D. F., & Shapiro, S. L. 1987, ApJ, 322, 113
Chernoff, D. F., & Weinberg, S. 1990, ApJ, 351, 121
Cudworth, K. C., & Hanson, R. B. 1993, AJ, 105, 168
Da Costa, G. S., & Armandroff, T. E. 1990, AJ, 100, 162
Dionidis, S. P., & Beers, T. C. 1989, ApJ, 340, L57
Eggen, O. J., & Iben, I. 1989, AJ, 97, 431
Fall, S. M., & Rees, M. J. 1984, MNRAS, 179, 541
Francois, P. 1991, A&A, 247, 56
Freeman, K. C. 1990, in Dynamics and Interaction of Galaxies, ed. R. Wielen (Heidelberg: Springer-Verlag), 36
Frenk, C. S., & White, S. D. M. 1980, MNRAS, 193, 295
Frogel, J. A., Persson, S. E., & Cohen, J. G. 1983, AJ, 53, 713
Geisler, D., Claria, J. J., & Minniti, D. 1991, AJ, 102, 1836
Geisler, D., Minniti, D., & Claria, J. J. 1992, AJ, 104, 627 (GMC)
Gratton, R. 1988, A&A, 177, 177
Gratton, R., & Ortolani, S. 1989, A&A, 211, 41 (GO)
Harris, W. E. 1975, ApJS, 29, 397
Holweger, H., Bard, A., Kock, A., & Kock, M. 1990, A&A, 232, 510
Holweger, H., Bard, A., Kock, A., & Kock, M. 1991, A&A, 249, 545
Kraft, R. P., Sneden, C., Langer, G. E., & Prosser, C. F. 1992, AJ, 104, 645
Kurucz, R. L. 1992a, Rev. Mexicana Astron. Af., 23, 45
———. 1992b, Rev. Mexicana Astron. Af., 23, 181
Laird, J. 1993, in The Globular Cluster–Galaxy Connections, ed. J. Brodie & G. H. Smith, in press
Laird, J., Rupen, M. P., Carney, R., & Latham, D. W. 1988, AJ, 96, 1908
Lambert, D. L., McWilliam, A., & Smith, V. 1992, ApJ, 386, 685
Leep, E. M., Oke, J. B., & Wallerstein, G. 1987, AJ, 92, 388
Majewski, S. R. 1992, ApJS, 78, 87
McClure, R. D., VandenBerg, D. A., Bell, R. A., Hesser, J. E., & Stetson, P. B. 1987, AJ, 93, 1144
McWilliam, A., Geisler, D., & Rich, R. M. 1992, PASP, 104, 1193
Minniti, D., Coyne, G. V., & Claria, J. J. 1992, AJ, 103, 871
Minniti, D., Peterson, R. C., Geisler, D., & Claria, J. J. 1993a, in The Globular Cluster–Galaxy Connection, ed. J. Brodie & G. H. Smith, in press
Minniti, D., Peterson, R. C., Geisler, D., DalleOre, C., & Claria, J. J. 1993b, in preparation
Morgan, S., & Lake, G. 1989, ApJ, 339, 171
Nomoto, K., et al. 1992, preprint
Peterson, R. C., & Carney, R. 1989, ApJ, 347, 266
Peterson, R. C., Kurucz, R., & Carney, B. 1990, ApJ, 350, 173
Pilachowski, C. A., Sneden, C., & Green, E. M. 1984, PASP, 96, 932
Ryan, S. G., & Norris, J. E. 1991, AJ, 101, 1865
Sandage, A. 1970, ApJ, 162, 841
Schuster, W. J., & Nissen, P. E. 1992, preprint
Sneden, C., Kraft, R. P., Prosser, G. F., & Langer, G. E. 1991, AJ, 102, 2001 (SKPL)
Stetson, P. B., & Harris, W. E. 1988, AJ, 96, 909
Suntzeff, N. B., Kraft, R. P., & Kinman, T. D. 1988, AJ, 95, 91
Trefzger, C., Carbon, D., Langer, G., Suntzeff, N., & Kraft, R. P. 1983, ApJ, 266, 144
VandenBerg, D. A., Bolte, M., & Stetson, P. B. 1990, AJ, 100, 445
Zhao, G., & Magain, P. 1990, AAS, 86, 85
Zinn, R. 1980, AJ, 42, 19
———. 1985, ApJ, 293, 424 (Z85)
Zinnecker, H., Keable, C. J., Dunlop, J. S., Cannon, R. D., & Griffiths, W. K. 1988, in IAU Symp. 126, The Harlow Shapley Symposium on Globular Clusters, ed. J. E. Grindlay & A. G. Davis Philip (Dordrecht: Kluwer), 603